

TESTS OF THIN-WALL DRIFT TUBES DEVELOPED FOR PANDA TRACKERS

A.P. Kashchuk, O.V. Levitskaya

The PANDA experiment will be carried out at the international FAIR facility in the GSI laboratory (Darmstadt, Germany). According to the Technical Design Report, the Forward Tracker (six stations FT1–FT6) [1] and the Central Straw Tube Tracker (STT) [2] will be composed from thin-wall drift tubes (called straw-tubes below) in large quantities, 13500 and 4600 tubes, respectively. The straw-tubes used here were produced by winding and gluing two Mylar aluminized films of 12 μm thickness (the wall thickness including the glue was $\sim 27 \mu\text{m}$). The tube wall was used as a cathode ($R_{\text{tube}} = 5 \text{ mm}$), and the coaxial gold-plated W-Re wire was used as an anode of the counter ($R_{\text{wire}} = 10 \mu\text{m}$). The Mylar material was preferred to the Kapton one because of its better mechanical properties – a higher Young’s modulus and tensile strength. The drift tubes are filled with two-component gas mixture Ar(90 %) + CO₂(10 %) at the 1 bar overpressure, *i.e.* at the 2 bar absolute gas pressure. The overpressure stretches the tube and prevents the wire sagging. The detector plane consisted of two mono-layers of drift tubes shifted by the radius R_{tube} , see Fig. 1a. The radiation length of a single tube X is characterized by $X/X_0 = 0.05 \%$, where X_0 is the media radiation length. As a calculation shows, the maximum sag of a 20 μm wire inside of a 1.5 m long horizontal straw tube due to its weight is smaller than 35 μm at the wire tension of 50 g.

In this report, we summarize various laboratory measurements made on straw tubes of 0.75 m and 1.5 m lengths (Fig. 1a), as well as on two module prototypes. The experimental set-up is shown in Fig. 1b. The modules were installed horizontally (as in the STT) and also vertically (as in the FT).

An intense 1.3 GBq ¹³⁷Cs γ -source (660 keV) was used for gas gain measurements, because a very low ionization current (pA) had to be detected. A low intensity ⁵⁵Fe X-ray source producing a point-like ionization in only one straw tube within the module was used for gas gain uniformity tests and to investigate the counting characteristics and cross-talks. A collimated ⁹⁰Sr β -source (emitting electrons of $\leq 2.3 \text{ MeV}$) with the intensity 11 MBq was used for efficiency measurements and for estimation of the spatial resolution of a single straw tube within the straw-module prototype.

The gas gain measurements were performed in order to specify the operational voltage at the 2 bar absolute gas pressure and to study the gas gain variations versus voltage, pressure, temperature and wire diameter. The ionization current corresponding to the unity gas gain was measured using the intense 1.3 GBq ¹³⁷Cs γ -source. In order to eliminate offsets in measurements of very small currents, we used batteries (as a floating voltage source) at both positive and negative voltages applied to the anode wire with respect to the cathode. The auto-ranging Keithley-485 pico-ammeter with the sensitivity of 0.1 pA was connected between the cathode and the ground. The ionization current $I_0 = 1.68 \pm 0.17 \text{ pA}$ was measured at $\pm 50 \text{ V}$ and $I_0 = 1.73 \pm 0.12 \text{ pA}$ at $\pm 100 \text{ V}$. The resulting value of $I_0 = 1.70 \pm 0.21 \text{ pA}$ was obtained by averaging the partial results. The gas gain at any voltage V was calculated as the ratio I/I_0 , where I was the current corresponding to the voltage V . Now the voltage was incremented in the range 1000–1900 V and the corresponding gas gain changed from 10^2 to 10^5 , see Fig. 2a.

The gas gain versus voltage at several gas overpressures (above the atmospheric pressure) at fixed temperature is presented in Fig. 2b. The results of measurements were fitted by the Diethorn formula with two parameters, E_{min} and ΔV [3]:

$$G(V, \rho) = \left[\frac{V}{a \ln(b/a) \cdot E_{\text{min}} \frac{\rho}{\rho_0}} \right] \frac{V}{\Delta V} \cdot \frac{\ln 2}{\ln(b/a)}. \quad (1)$$

Here, a and b are the radii of the anode wire and cathode tube, respectively, E_{min} is the minimal electric field needed for ionization, ΔV corresponds to the minimal voltage difference required to produce free electrons in an avalanche; $\rho/\rho_0 = (P/T)/(P_0/T_0)$ and P/T are the ratios of gas density, pressure and temperature at the real conditions to the reference ones $P_0 = 1000 \text{ mbar}$, $T_0 = 293 \text{ K}$, respectively.

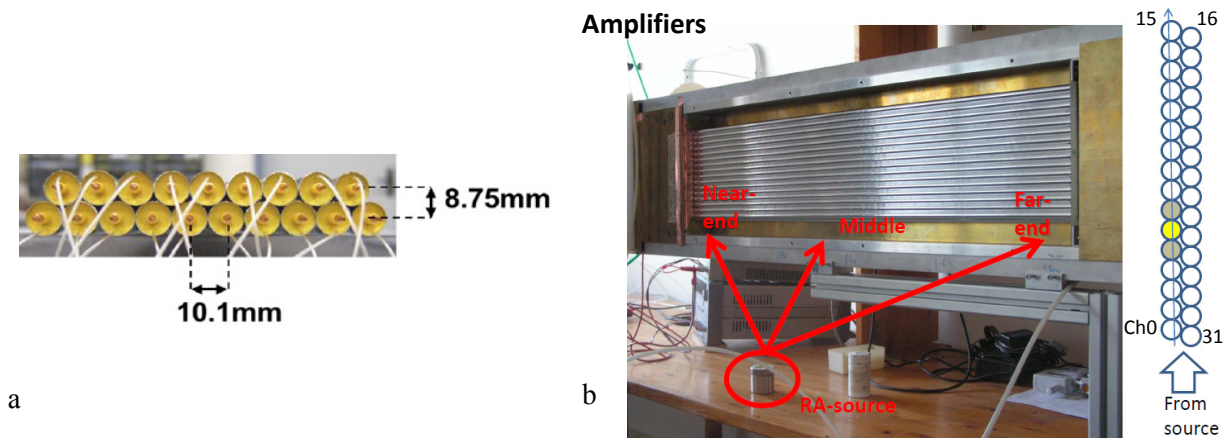


Fig. 1. Two mono-layers of thin-wall drift tubes filled with Ar(90 %) + CO₂(10 %) mixture at the 2 bar absolute gas pressure (a) and double layer 32-straw module prototype used in laboratory tests with various radioactive sources (b)

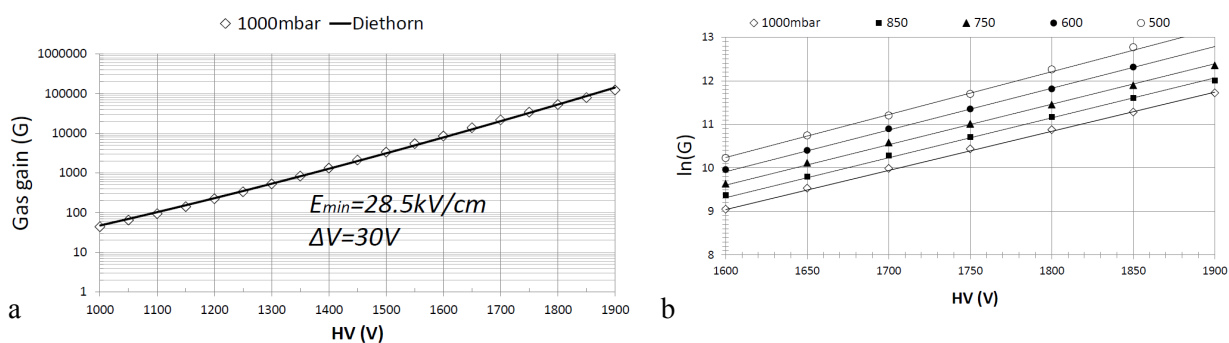


Fig. 2. Gas gain vs voltage for Ar(90 %) + CO₂(10 %) gas mixture at the 1000 mbar overpressure, (at the 2 bar absolute gas pressure) and the Diethorn parametrization of the measurement results (a). The gas gain vs voltage at various gas overpressures ranged from 1000 mbar down to 500 mbar (b). The points correspond to the measurements, the lines – to the parameterization function

Tests with the ⁵⁵Fe-source were performed to find a set of characteristics. In these measurements, the straw-tube impedance was terminated with the amplifier impedance via a 350 Ohm resistor connected in series to the amplifier, while the far-end of the straw-tube was un-terminated [4]. In Fig. 3a, a typical amplitude spectrum is presented, which was used to verify the gas gain uniformity along the straw-tube. In the case of an individual straw tube, the sag can modify the gas gain dramatically in the middle of the tube. But for the 32-straw module where the tubes were arranged in double layer and glued together, the gas gain is rather uniformly distributed. In this case the gas gain non-uniformity in the middle of any tube within the module is below 1 %, as it is shown in Fig. 3b.

Figure 4a shows three typical regions observed in the counting characteristics measured with the ⁵⁵Fe-source: the beginning of the plateau (the point corresponding to 5.9 keV), the constant rate region (the plateau) and the region of increasing counting rate above the end of the plateau. The measurements show rather similar counting rates for all straw tubes within the 32-straw module in all regions mentioned above: at the near-end (at the amplifier side), in the middle and at the far-end. The rise of the counting rate correlates with the growth of the dark current and appearance of two and more pulses (cross-talks). The position of the plateau end strongly depends on the quality of straw-tube production. The ⁵⁵Fe X-ray source produces point-like ionization in the gas and generates signals in one and only one straw tube. This feature makes possible to measure the cross-talks in any pair of tubes within the module. As is shown in Fig. 4b, typical cross-talks were observed on the level of 0.2 % in a wide range of voltages up to 1900 V in some cases, and only near the end of the plateau they could reach 10 % and even 100 %.

The efficiency of particle detection was measured with the collimated ^{90}Sr -source with the aim to specify the operational voltage for registration of MIPs (minimum ionizing particles). The particles emitted by the ^{90}Sr -source cross many tubes, as illustrated in Fig. 5a. A set of three neighboring tubes was used to find the efficiency of the inner tube with respect to the outer tubes. The efficiency was measured at both ends and in the middle of the tube. Figure 5a shows the efficiency versus voltage at a fixed threshold of 10 fC. Figure 5b shows the dependence of the efficiency on the threshold for several voltages.

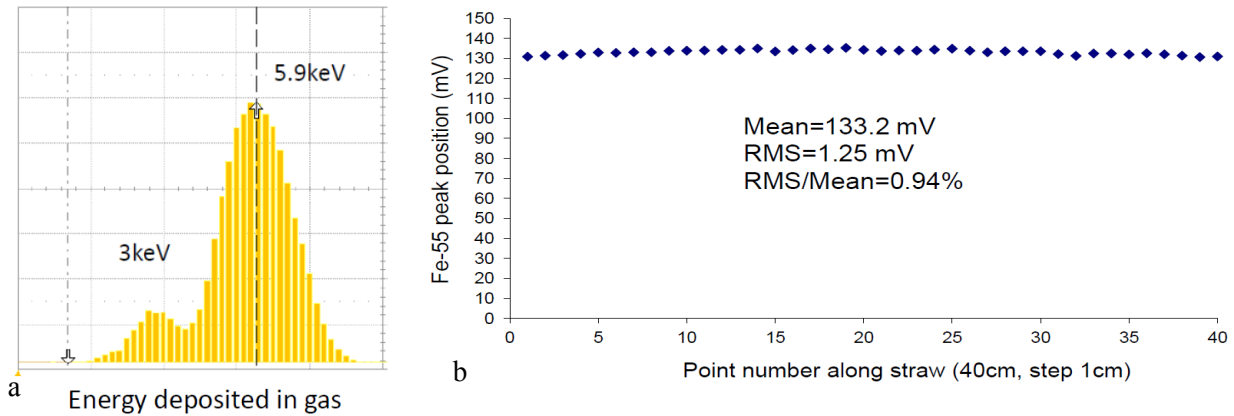


Fig. 3. Typical amplitude spectrum measured with the ^{55}Fe -source in a single tube within a 32-straw module (a). Gas gain variation in the tube measured as the position of the 5.9 keV peak along the distance of 40 cm in the middle of the tube (b)

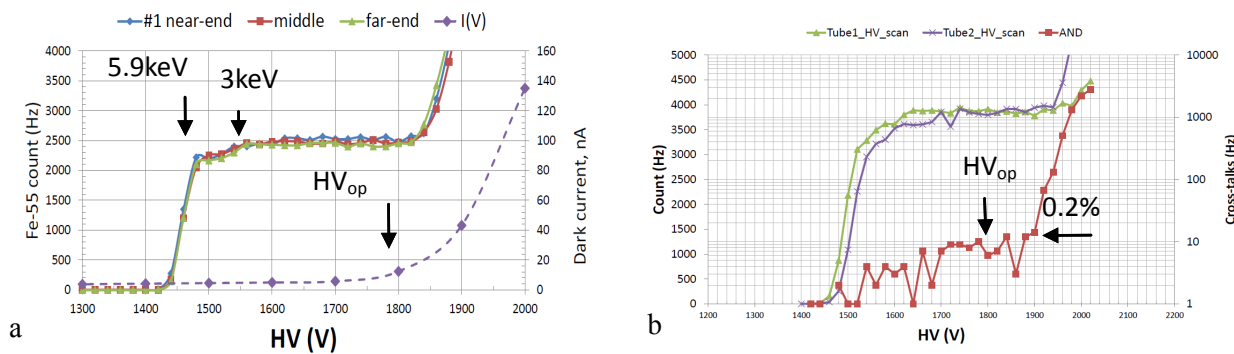


Fig. 4. Counting characteristics measured with the ^{55}Fe -source at a sequence of points along a 0.75 m straw tube filled with Ar(90 %) + CO_2 (10 %) mixture at the 2 bar absolute gas pressure (a). The cross-talks measured with the ^{55}Fe -source between two straw tubes of 1.5 m length (b). $\text{HV}_{\text{op}} = 1800 \text{ V}$ is indicated as the operational voltage for registration of MIPs

We have compared the results of the efficiency measurements obtained with the ^{90}Sr -source and with Cosmic Rays (CR), performed at large statistics, collected for many days, for all straw tubes within the 32-straw module. The measurements with CR were made at the $\text{HV} = 1800 \text{ V}$ (Fig. 6a) and $\text{HV} = 1700 \text{ V}$ (Fig. 6b). One can notice that the results obtained with ^{90}Sr and CR are consistent. Comparing the data in Figs. 5a, b and 6a, b we see that the operational voltage should be at least 1800 V. According to Fig. 2a, the gas gain at the $\text{HV} = 1800 \text{ V}$ is equal to 5.5×10^4 . A similar gas gain at the $\text{HV} = 1800 \text{ V}$ was obtained in a cross-check using the ^{55}Fe -source by measuring both the rate (see the plateau in Fig. 4a) and the current. If the gas gain is known, we can map the threshold of 10 fC to 10 p.e. (primary electrons). Then, the efficiency with such a threshold has to be better than 95 % at 200 p.e./cm, which is the total number of primary electrons formed along the track of a MIP at the 2 bar absolute gas pressure, assuming a uniform distribution of primary clusters along the track. In reality, the efficiency will be better and close to 100 % in a 2-layer detector.

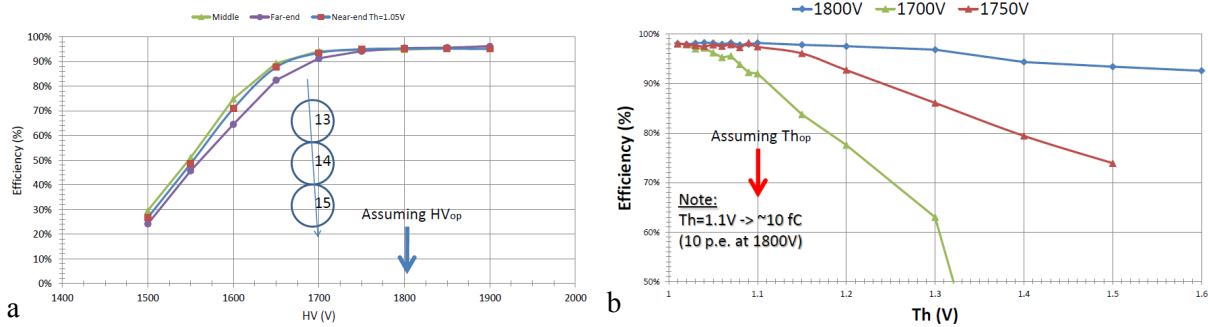


Fig. 5. Efficiency vs voltage at a fixed threshold for various points along a straw tube (a), and efficiency vs threshold at fixed voltages at the wire (b). Both characteristics were obtained in few minutes with the ^{90}Sr -source using the “three neighbouring tubes” method

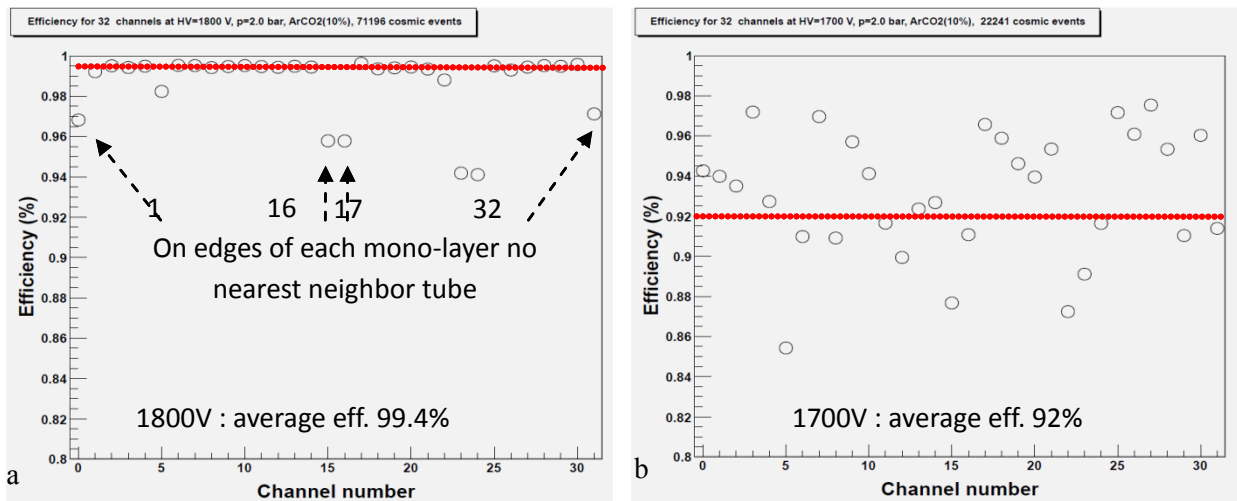


Fig. 6. Efficiency of straw tubes within a 2-layer (16 + 16 = 32 straw) module at the HV = 1800 V (a) and HV = 1700 V (b) obtained with CR with large statistics collected for many days

Further tests were performed to estimate the single-straw spatial resolution by observation of time spectra. The time-to-digit conversion was made with a 128-channel CAEN TDC module V1190A with the time resolution 100 ps/bin. Our ^{90}Sr source of charged particles for laboratory tests is a unique one, it allows to obtain large statistics in a few minutes (10^5 events in 20 min), while many days are required with CR. Nevertheless, this source is not appropriate for accurate measurements of the spatial resolution due to low energies of electrons (maximum 2.3 MeV), because significant multiple scattering in the gas and material of the detector deteriorates its spatial resolution.

Measurements of TDC-spectra with ^{90}Sr were carried out at the operational voltage of 1800 V and threshold 10 p.e. As one can see in Fig. 7a, b, primary electrons drift without multiplication practically through all the distance R_{tube} . Avalanches in the gas start at the distance $r \approx 102 \mu\text{m}$ from the anode wire, at the electric field $E_{\text{min}} = 28.5 \text{ kV/cm}$, as is shown in Fig. 2a.

Raw TDC-spectra measured with the ^{90}Sr -source are “corrupt” due to two main processes. The first process is clusterization of primary ionization along the track, the second is multiple scattering of low energy electrons emitted by ^{90}Sr . As it is illustrated in Fig. 8a, b, many primary electrons drift to the wire from the track with different starting velocities, and they can produce two or more pulses (hits). The first pulse is used as a rule to determine the spatial coordinate. However, the second pulse from the same track (or even the 3-rd) can be also registered with a multi-hit TDC. As one can see in Fig. 9a, b in the two-dimensional plot and its projections, low energy electrons scattered in the gas, on the wall and also on the glue can randomly “deform” the shape of the TDC-spectrum. In such a case, the 1-st pulse can be wrong, *i.e.* it can be not related to the closest electron cluster to the wire.

The spatial resolution of a single straw-tube was obtained using the so-called “auto-calibration” technique described in detail in [2]. Parameters of the TDC-spectrum and the corresponding $r(t)$ -relation (Fig. 10a, b) for each channel were derived from a fit performed with the following empirical function:

$$\frac{dn}{dt} = p_1 + \frac{p_2[1 + p_3 \exp((p_5 - t) / p_4)]}{[1 + \exp((p_5 - t) / p_7)][1 + \exp((t - p_6) / p_8)]}. \quad (2)$$

Here, dn is the number of events within the time bin dt in the TDC-spectrum, the parameters p_5 and p_6 are the values t_{\min} and t_{\max} , their difference being the maximum drift time in the straw-tube; other parameters describe the spectrum shape.

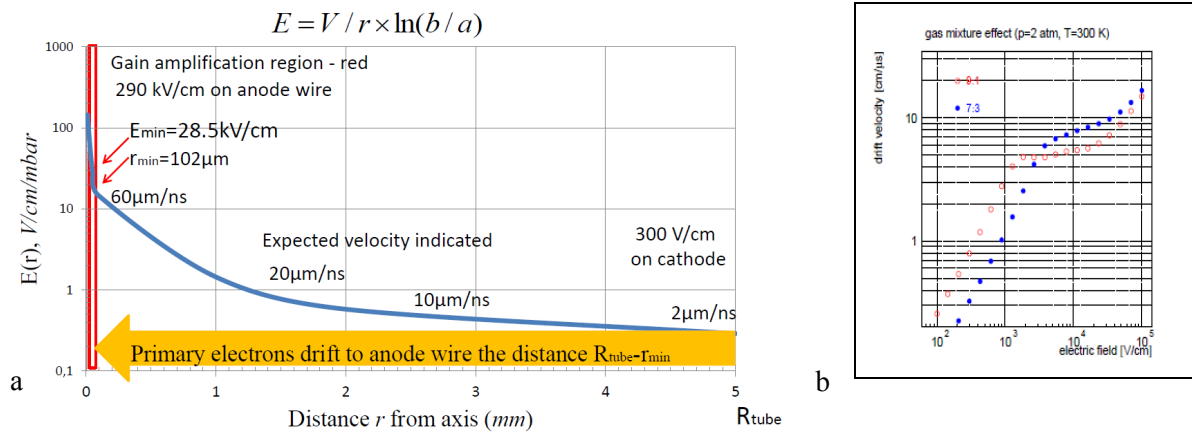


Fig. 7. Electric field strength in a tube at 1800 V with indication of the electron drift velocities at certain field values (a). Electron drift velocity vs electric field for two-component gas mixtures Ar + CO₂ at the 2 bar gas pressure [2]: open red points – our case of Ar(90 %) + CO₂(10 %), blue points – Ar(70 %) + CO₂(30 %) (b)

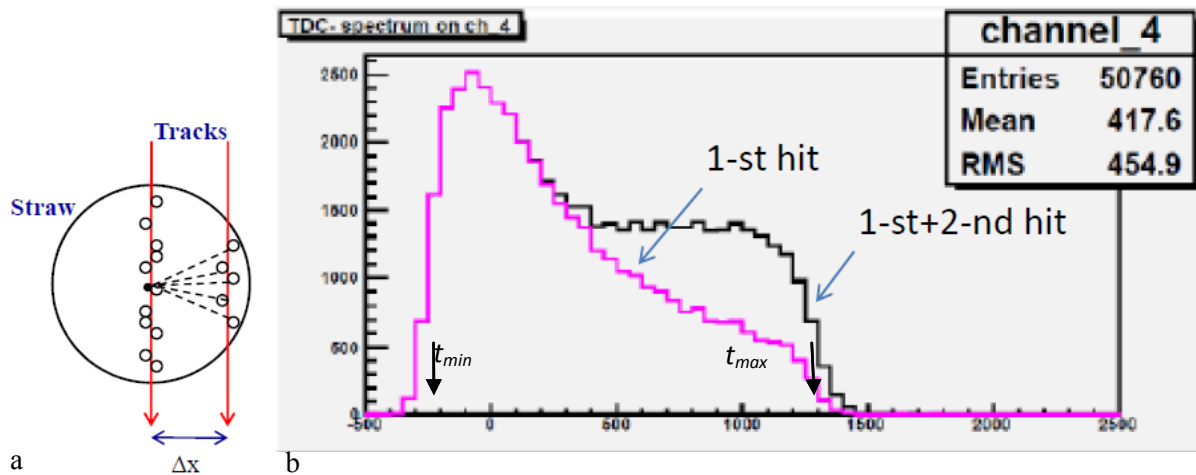


Fig. 8. Origin of multiple pulses due to clusterization of primary ionization along the track (a); TDC-spectrum measured with the ⁹⁰Sr-source including only the 1-st pulse and a sum of the 1-st and 2-nd pulses (b). With multiple scattering, the 1-st pulse can be generated by a cluster not nearest to the wire. The time scale is in the TDC sampling units, one histogram bin containing 50 sampling units

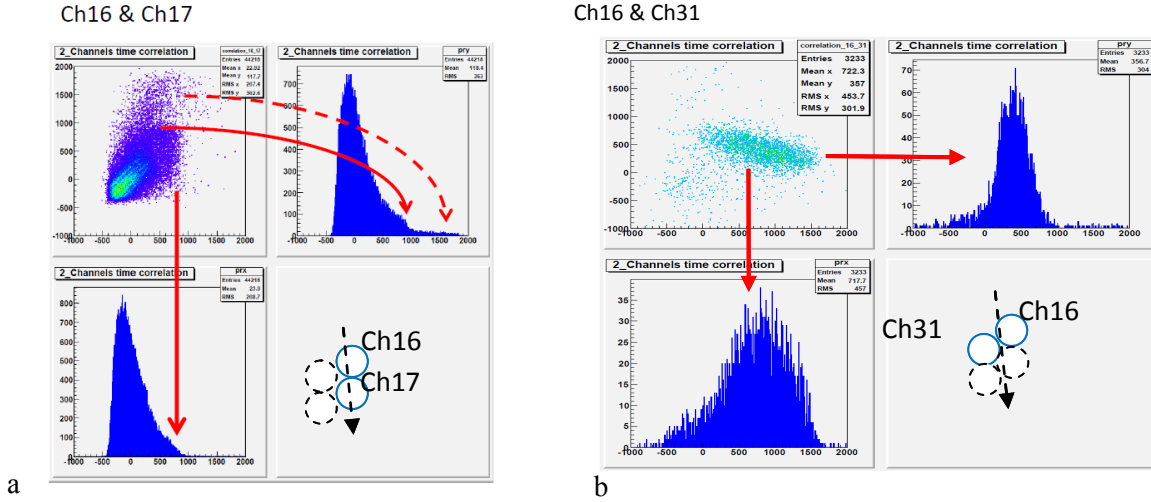


Fig. 9. 2D plot of the correlation between two time intervals for two tubes Ch16 and Ch17 from the same straw monolayer, measured with the ^{90}Sr -source with TDCs, and the 1D TDC-spectra obtained as its projections (a). The same plot for another pair of tubes Ch16 and Ch31 taken from different monolayers (b). The tails, as well as spurious hits on the level of $\sim 20\%$ in the TDC-spectra, appear due to multiple scattering. To obtain correct TDC-spectra and the $r(t)$ -relation, a special hit selection is provided in the event analysis

The $r(t)$ -relation has been found from the TDC-spectrum with N_{tot} entries using the following formula:

$$r(t) = \int_{t_{\min}}^{t_{\max}} \frac{dr}{dt} \cdot \frac{dn}{dn} = \frac{R_{\text{tube}} - R_{\text{wire}}}{N_{\text{tot}}} \int_{t_{\min}}^{t_{\max}} \frac{dn}{dt} \approx \frac{\sum_{i=1}^{i=t} n_i}{N_{\text{tot}}} \cdot (R_{\text{tube}} - R_{\text{wire}}). \quad (3)$$

For further conversion from the measured time to spatial coordinate, the $r(t)$ -relation was parameterized by the Chebyshev polynomial of the 5-th order:

$$r(t) = q_0 + q_1 t + q_2 (2t^2 - 1) + q_3 (4t^3 - 3t) + q_4 (8t^4 - 8t^2 + 1) + q_5 (16t^5 - 20t^3 + 5t). \quad (4)$$

Here, t is the time interval measured as the radius of an isochrone, *i.e.* the distance from the primary cluster to the wire; the parameter q in Fig. 10b has been replaced by p .

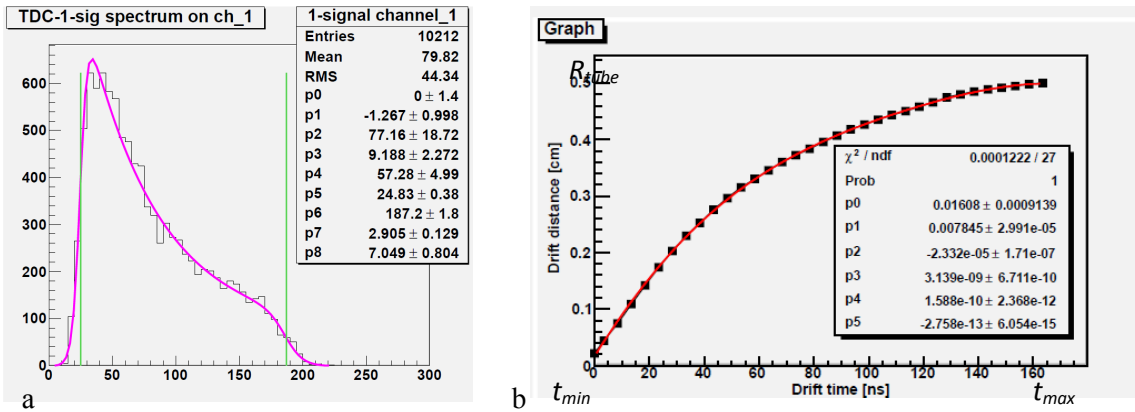


Fig. 10. TDC-spectrum measured with the ^{90}Sr -source for one straw tube (time in ns) (a), and the corresponding $r(t)$ -relation with the parameters (b)

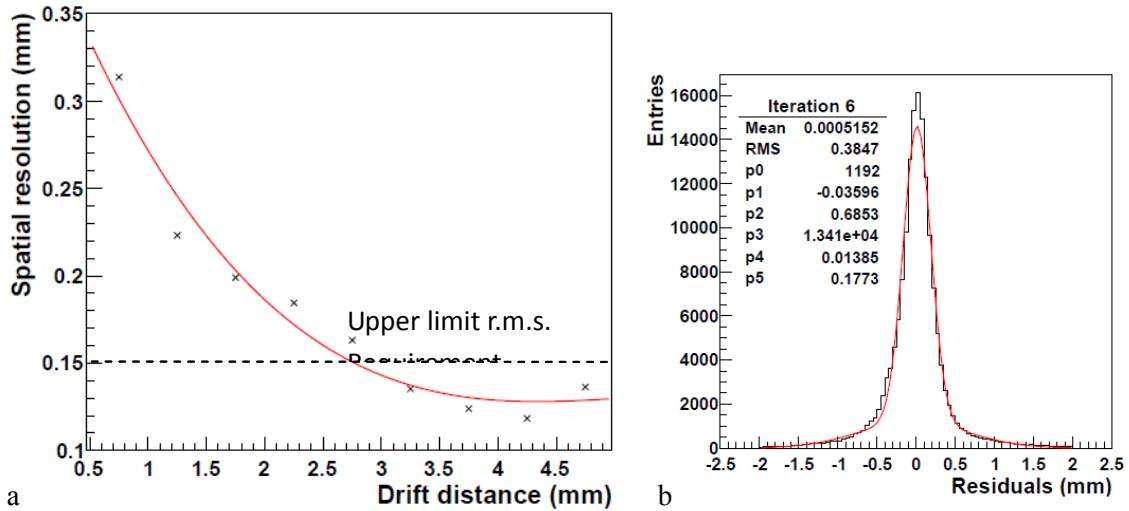


Fig. 11. Spatial resolution measured with the ^{90}Sr -source as a function of the distance between the track and the wire (a). The averaged distribution of residuals and its r.m.s., $p5 = 177.3 \mu\text{m}$ (b). The spatial resolution specified for the PANDA experiment is indicated by the dashed line

According to the auto-calibration, the final $r(t)$ -relation is obtained sequentially by iterations using various hit selection criteria. The residuals, which are the differences between the best track and $r(t_i)$, are minimized by this iterative procedure (t_i is the measured time interval in the i -th TDC-channel).

As one can see in Fig. 11a, a much better spatial resolution is obtained in the region from $R_{\text{tube}}/2$ to R_{tube} within each mono-layer shifted by R_{tube} if the data are not averaged over the full interval R_{tube} . Using this effect, one can combine the data properly from two independent monolayers in order to improve the spatial resolution.

The upper limit of the spatial resolution specified for the PANDA experiment is $150 \mu\text{m}$ (r.m.s.). According to the TDR, the resolution like that will provide the momentum resolution of the order of 1 %.

A large spread of the parameters of Eq. (2) describing the TDC-spectra of the 32-straw module was observed due to multiple scattering of low energy electrons, emitted by ^{90}Sr in a wide energy range around 2 MeV. As could be expected, this explains why the spatial resolution measured with the ^{90}Sr -source is worse than that predicted by simulations, see Figs. 11a, b and 12a, b, c.

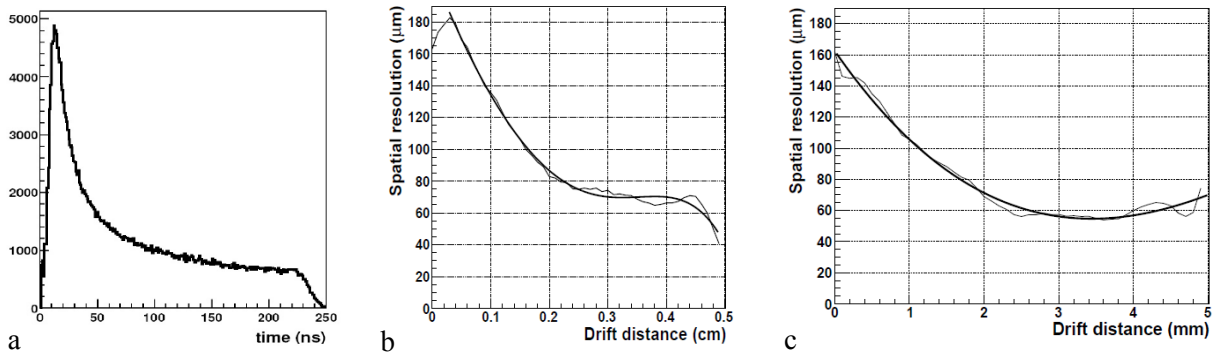


Fig. 12. Simulation of a TDC-spectrum for MIP particles. As the simulation shows, the magnetic field extends the drift time to 220 ns (a). Single straw-tube spatial resolution (r.m.s.) vs distance to the wire found without a magnetic field (b) and with a magnetic field (c). In the range between $R_{\text{tube}}/2$ and R_{tube} , the resolution is around $70 \mu\text{m}$ (r.m.s.). These results were taken from [2, 5]

Our goal at present is to prepare the apparatus, technique and software for beam tests with high energy particles at various rates with and without magnetic fields and to compare the results of measurements with

simulations. Note that tests with radioactive sources are good tools for straw-tube quality control at the mass production and provide feedback on possible improvements of the module assembly procedures.

This work was performed in collaboration with P. Gianotti and M. Savrie.

References

1. PANDA Forward Tracking System. Technical Design Report (in preparation).
2. PANDA Central Straw Tube Tracker. FAIR/Pbar/Technical Design Report, Darmstadt (2012), http://panda-wiki.gsi.de/pub/Tracking/WebHome/panda_tdr_trk.pdf
3. P. Gianotti, A. Kashchuk... O. Levitskaya *et al.*, Note LNF-**11/05** (P), Frascati (2011).
4. A.P. Kashchuk... O.V. Levitskaya *et al.*, Phys. of Particles and Nuclei Letters **8**, 40 (2011).
5. S. Costanza... A. Kashchuk... O. Levitskaya *et al.*, Nuovo Cim. **34** C, 94 (2011).